

MeV ion confinement in the TFTR tokamak*

S. J. Zweben,[†] R. L. Boivin, R. E. Duvall, E. D. Fredrickson, R. J. Goldston, H. E. Mynick, J. D. Strachan, and R. B. White
Princeton Plasma Physics Laboratory, Princeton, New Jersey 08543

(Received 4 December 1989; accepted 21 February 1990)

In this paper the confinement of the MeV ions that are created by D–D reactions in the TFTR tokamak [in *Plasma Physics and Controlled Nuclear Fusion Research 1988* (IAEA, Vienna, 1989), Vol. 1, p. 27] is described. The ions that escape from the plasma are measured by a new type of detector located just outside the plasma edge. Most measurements made with this detector are consistent with the first-orbit loss of these ions. Exceptions are correlated with strong magnetohydrodynamic activity, and a preliminary explanation is presented.

I. INTRODUCTION

This paper describes measurements of the confinement of the D–D alpha-like fusion products in TFTR (the Tokamak Fusion Test Reactor at PPPL).¹ These results can help to form a baseline for evaluating alpha particle confinement in future D–T tokamaks.

The D–D MeV ions of interest here are the 1.0 MeV triton and the 3.0 MeV proton, which are made in equal numbers to the 2.5 MeV neutron. For typical TFTR neutron production rates of $> 10^{16}$ n/sec, up to 10 kW of power is created in these ions. This MeV ion population is large enough to readily measure, but still small compared with the $1000\times$ larger alpha populations expected at TFTR's D–T goal of $Q \approx 1$. Note that the gyroradii of the tritons and protons are equal to each other and very nearly equal to that of the 3.5 MeV alpha, which makes these D–D ions suitable for tests of alpha confinement physics.

The physics of MeV ion confinement can be divided into three areas. The simplest area concerns the neoclassical confinement effects, which for MeV ions in TFTR are dominated by the large-banana first-orbit loss. The second area concerns the effects of nonaxisymmetries on the ion confinement, particularly those resulting from internal magnetohydrodynamic (MHD) activity and externally imposed toroidal field ripple. The third and most difficult area concerns the possible collective effects that large populations of MeV ions (i.e., alphas or possibly ion cyclotron generated minority tail ions) might have on the plasma, or on their own confinement. This paper describes results pertaining to the first two areas only.

The neoclassical effects expected for tritons in TFTR are fairly simple. A typical triton banana width for TFTR at a low current ($I \approx 1$ MA) is $\Delta_T \approx q(R/r)^{1/2} \rho_{\text{tor}} \approx 30$ cm, which is about half the plasma minor radius of $a = 80$ cm (where q is the local magnetic safety factor, r is the local minor radius, R is the major radius, and ρ_{tor} is the toroidal gyroradius). Thus at low current a significant fraction of tritons should be lost from the plasma on their first orbits, and with increasing plasma current this first-orbit loss

should decrease, since the triton banana width decreases. Tritons that are lost on their first orbit should also be lost "promptly" with nearly their birth energy ($1 \text{ MeV} \pm 20\%$ Doppler shift), since the loss time ($\approx 1 \mu\text{sec}$) is negligible compared to their thermalization time ($\lesssim 1$ sec).

II. EXPERIMENTAL RESULTS

MeV ion detectors have been installed on TFTR to measure these first-orbit losses. The detector used for the present experiment was located near the vessel wall about 90° poloidally below the outer midplane, and was capable of measuring the triton flux versus energy (in the range 0.5–3 MeV), pitch angle (in the range 40° – 90° with respect to B in the "co-"going direction), and time (up to 20 kHz). The design consists of a pinhole/slit aperture pair that disperses ions according to their gyroradius in one dimension (similar to a magnetic spectrometer) and their pitch angle in the other dimension. The impact of these ions onto a ZnS (Ag) scintillator screen is measured by an optically coupled two-dimensional (2-D) imaging system, similarly to a prototype discussed previously.²

Note that although the tritons and protons are measured together we will call this the "triton" signal, since $\sim 75\%$ of the scintillator light is expected to come from the tritons (the 0.8 MeV ^3He ions are filtered out by the $3 \mu\text{m}$ foil used to block plasma light). The main background in this system is due to light created in the fiber bundle itself by neutrons and gammas, which is proportional to the global neutron flux and easily subtracted out.

The expected triton first-orbit loss into this detector was determined using a Lorentz code developed for this purpose at PPPL. This code calculated the flux versus pitch angle (as measured at the detector) by following the orbit trajectories backward into the plasma and integrating over the assumed triton source profile. At a given current the expected flux peaks sharply at the pitch angle of the "fattest" banana orbit, typically at about 60° with respect to B in the co-going direction, since the trajectory of that orbit comes closest to the high triton source region near the plasma center.² At a given pitch angle the expected flux decreases with plasma current, since the trajectory moves farther from the plasma center. These qualitative expectations are relatively insensitive to the assumed triton source and plasma current profiles.

*Paper 613, Bull. Am. Phys. Soc. 34, 2074 (1989).

[†] Invited speaker.

The experimental results for MHD-quiet discharges are summarized in Figs. 1 and 2.

Figure 1 shows 2-D images of light from the scintillator for six different plasma currents, each image taken with a 4 msec exposure time during neutral beam injection (NBI) when the neutron flux was $4.5 \pm 0.5 \times 10^{15}$ n/sec. The triton signal intensity is represented by a false-color scale only approximately visible here, with the area of the dark regions roughly proportional to the intensity. The images are oriented so that the low gyroradius tritons are downward and low pitch angle tritons are to the left.

These experimental results are consistent with the first-orbit loss model in several respects. First, the triton energy inferred from the peak in the gyroradius distribution is always near to the triton birth energy of 1 MeV, as expected for first-orbit loss (as indicated for the 1.2 MA case). Second, the triton pitch angle distribution is peaked near 60° , as expected for the fattest banana orbit (also indicated for the 1.2 MA case). Third, the total triton flux (at fixed neutron source strength) decreases with increasing plasma current by about $3 \times$ over the range 0.9–1.4 MA, roughly agreeing with first-orbit code calculations (the absolute flux is also roughly consistent with this model²). Note that the observed width of these distributions of about ± 0.5 MeV and $\pm 20^\circ$ are roughly consistent with the expected geometrical apertures and optical resolutions of the detector.

The typical time dependence of the triton flux is shown in Fig. 2. This triton signal comes from a phototube coupled to the brightest region of the scintillator, and the neutron signal comes from a standard TFTR epithermal neutron detector. In discharges without strong MHD, the time dependence of the triton signal follows that of the neutron signal, as expected for prompt first-orbit loss. Similar behavior is observed in all MHD-quiet discharges at plasma currents from 0.8–1.6 MA and neutron rates from $\approx 10^{15}$ – 3×10^{16} n/sec.

III. MHD EFFECTS

When strong coherent MHD activity is present, the average triton signal can increase by up to $5 \times$ above the first-orbit loss level, as shown in Fig. 3. The discharge of Fig.

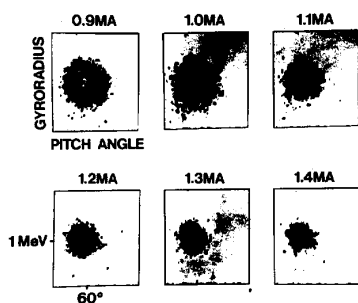


FIG. 1. Video camera images of the triton-detection scintillator screen taken during NBI at six different plasma currents. Each image was exposed for 4 msec at a time when the neutron rate was $4.5 \pm 0.5 \times 10^{15}$ n/sec. The area of the dark regions is approximately proportional to the triton flux. The inferred triton energy, pitch angle, and current dependence are consistent with first-orbit loss calculations.

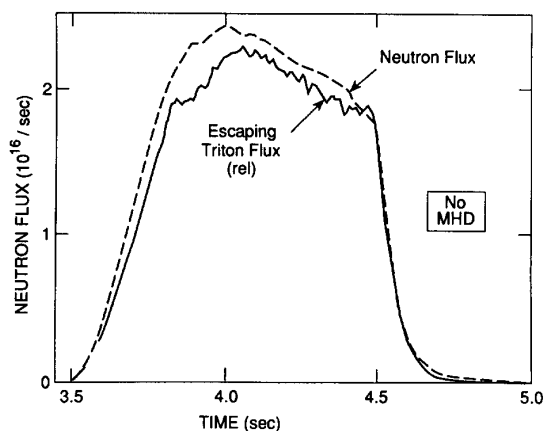


FIG. 2. Typical time dependence of the escaping triton flux during a MHD-quiet discharge. The triton signal comes from a phototube monitoring the peak triton flux at the scintillator. The neutron rate is normalized to the triton signal at 4.5 sec, showing the similarity of the time dependence of the triton source rate and the escaping triton flux. This discharge was at 1.6 MA and 25 MW NBI (shot #37915).

3 is similar to that of Fig. 2, except that the slightly larger beam power in Fig. 3 induced strong MHD activity between 3.8 and 4.3 sec (note that the normalization of triton to neutron signals is the same as for Fig. 2).

An examination of the time dependence of the escaping triton flux during coherent MHD activity always shows the triton flux to be fluctuating at the same frequency as the MHD mode measured with external \vec{B} loops or internal \vec{T}_e , as shown, for example, in Fig. 4. Such coherent triton oscillations have been observed over a range of frequencies 1 – 10^4 Hz, with mode structures $m = 1$ – 4 ($n = 1$), and amplitudes $\vec{B}_p/B_p \approx 0.1\%$ – 1% (at the wall), which constitute about 30% of the high-power NBI discharges in TFTR. The maximum triton flux is up to a factor of 10 times the first-orbit loss level (as observed without MHD). Note that the global

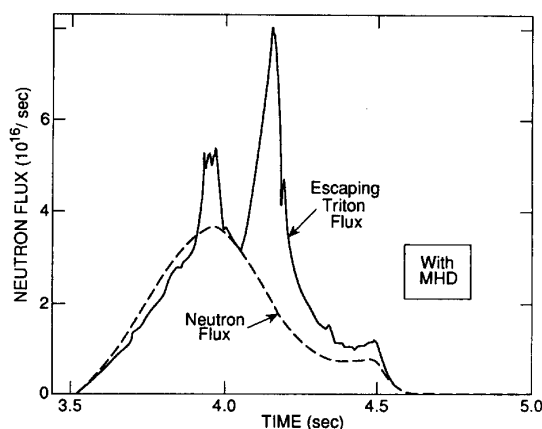


FIG. 3. Typical time dependence of the escaping triton flux during a discharge with strong MHD activity during the period 3.8–4.3 sec. The escaping triton flux increases dramatically during MHD activity. The normalization of the neutron signal to the triton signal is the same as for Fig. 3. This discharge was at 1.6 MA and 30 MW (shot #37913).

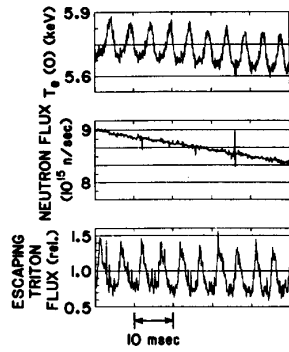


FIG. 4. Example of the detailed time dependence of escaping triton flux compared to the MHD activity as monitored by the internal electron temperature fluctuations. The triton flux increases in phase with the mode, which in this case was an $m = 2, n = 1$ mode in a 1.4 MA discharge at 23 MW NBI power. The triton flux does not decrease below the first-orbit loss level, and the neutron flux does not fluctuate perceptibly.

neutron source strength does not fluctuate perceptibly during coherent MHD activity.

What causes this enhanced triton loss during coherent activity? The most likely explanation involves an internal radial “kick” of the previously confined countergoing triton orbits due to the MHD mode. In particular, if a confined countergoing triton passes through a region of the mode with an inward radial magnetic field, its orbit can be kicked radially outward, even if the particle energy and magnetic moment are unchanged. If this confined orbit was originally near the passing/trapped boundary, it could be converted into an unconfined banana orbit such as those normally lost into our detector.

Computer simulations of this process have been made using a guiding center code with an $m = 3, n = 2$ magnetic island.³ The results are at least qualitatively similar to the experimentally observed behavior described above, namely, that the triton flux to the detector is increased by some factor (3–5) when the mode phase is chosen properly with respect to the detector. Efforts are underway to quantitatively test this model, particularly with respect to the phase angle between the triton and MHD fluctuations.

What about the effects of other plasma fluctuations on triton confinement?

Occasionally a sudden increase in the triton flux by a factor of ≈ 10 is observed during a sawtooth crash. This may be caused by similar “kick” of the confined tritons across the passing/trapped boundary, except that here the kick would come infrequently, and only near the $q = 1$ surface. A simple estimate of the sawtooth-induced lost triton flux can be made by assuming that all the confined tritons within a radial width δ_{st} (just inside the $q = 1$ surface), and with a magnetic moment observable from the detector, are expelled across the passing/trapped boundary on orbits near the usual first-orbit loss trajectory:

$$\frac{\Gamma_{st}}{\Gamma_{fo}} \approx \frac{\tau_{slow} \delta_{st}}{\tau_{st} \Delta_{det}}, \quad (1)$$

where Γ_{st} is the triton flux lost near the trapped/passing

boundary during the sawtooth crash time τ_{st} (≈ 0.1 msec), Γ_{fo} is the triton first-orbit loss without MHD as observed by the detector viewing a minor radial region Δ_{det} (≈ 10 cm) near the trapped/passing boundary, and τ_{slow} is the typical time a confined triton takes to slow down below the detection threshold (≈ 0.5 sec). Note that the normalization to first-orbit loss introduces the detector radial integration width in the denominator, and that the fraction of triton velocity space seen by the detector is assumed to be the same for first-orbit and sawtooth-induced losses. Assuming only $\delta_{st} \approx 1$ cm implies that the triton flux should increase by roughly a factor of 10^3 during the sawtooth crash, which is larger than the observed factor of 10 (possibly because of a nonaxisymmetry of the kicks).

IV. DIFFUSIVE EFFECTS

How would small-scale turbulence affect the triton confinement? If this turbulence resulted in a radial triton diffusion coefficient D_T for counterpassing confined tritons near the passing/trapped boundary, the steady-flux of diffusing tritons Γ_D having a magnetic moment visible from our detector could be estimated as

$$\Gamma_D / \Gamma_{fo} \approx D_T \tau_{slow} / (L_T \Delta_{det}), \quad (2)$$

where L_T is the radial scale length of the confined triton population that could diffuse into the detector (note that the normalization to first-orbit loss again introduces the detector integration width Δ_{det} and causes the velocity-space fraction to drop out). Since the population of tritons at the passing/trapped boundary is zero, L_T is most likely set by the triton diffusion process itself⁴ to be $L_T \approx (D_T \tau_{slow})^{1/2}$.

The implication of this argument is that a D_T comparable to that of the thermal background plasma D_{th} (≈ 5000 cm²/sec) should produce a substantial increase in the triton flux above the first-orbit level. If we assume a D_T of only 100 cm²/sec, the expected triton flux should increase about 50% above the first-orbit level after a slowing-down time scale of about 0.5 sec, and should decrease slowly over the same time scale after NBI, in contrast to the observed behavior triton flux, which is proportional to the triton (i.e., neutron) source rate, as shown in Fig. 2.

Such a low triton diffusion coefficient can be understood in terms of the Mynick–Krommes–Strachan model of “orbit averaging” for diffusion of large gyroradius particles in a background spectrum of small-scale turbulence.⁵ For electrostatic turbulence with $k_1 \rho_T \approx 1$ and $k_1 \Delta_T > 1$, where k_1 is the radial mode wavenumber, ρ_T is the triton gyroradius, and Δ_T is the triton banana width, this model predicts the triton diffusion rate, normalized to the background thermal ion diffusion, to be

$$D_T / D_{th} \approx (k_1 \rho_T)^{-1} (k_1 \Delta_T)^{-2}. \quad (3)$$

For TFTR we can estimate $k_1 \rho_T \approx 10$ and $k_1 \Delta_T \approx 60$, so that the calculated triton diffusion is $D_T < 100$ cm²/sec, roughly consistent with experiment. A similar argument could be made assuming small-scale magnetic fluctuations.

A major piece of triton confinement physics that has not yet been studied with this system is the possible diffusion of confined *trapped* tritons, such as could be produced by non-

axisymmetric toroidal field or MHD-induced "ripple."⁶ Such diffusion tends to result in triton loss concentrated near the outer midplane region⁷ and will be studied by a new midplane triton detector presently being installed on TFTR. Such loss processes might explain anomalies in the triton burnup measurements previously reported on TFTR.⁸

ACKNOWLEDGMENTS

We thank C. E. Barnes and J. Felt for work on the orbit code, and K. M. Young and D. Meade for their support of these experiments.

This work was supported by the U.S. Department of Energy Contract No. DE-AE02-76-CHO3073.

¹M. G. Bell, V. Arunasalam, C. W. Barnes, M. Bitter, H.-S. Bosch, N. L. Bretz, R. Budny, C. E. Bush, A. Cavallo, T. K. Chu, S. A. Cohen, P. L. Colestock, S. L. Davis, D. L. Dimock, H. F. Dylla, P. C. Efthimion, A. B. Ehrhardt, R. J. Fonck, E. D. Fredrickson, H. P. Furth, G. Gammel, R. J. Goldston, G. J. Greene, B. Grek, L. R. Grisham, G. W. Hammett, R. J. Hawryluk, H. W. Hendel, K. W. Hill, E. Hinnov, J. C. Hosea, R. B. Howell, H. Hsuan, R. A. Hulse, K. P. Jaehnig, A. C. Janos, D. L. Jassby,

F. C. Jobs, D. W. Johnson, L. C. Johnson, R. Kaita, C. Kieras-Phillips, S. J. Kilpatrick, V. A. Krupin, P. H. LaMarche, W. D. Langer, B. LeBlanc, R. Little, A. I. Lysojvan, D. M. Manos, D. K. Mansfield, E. Mazzucato, R. T. McCann, M. P. McCarthy, D. C. McCune, K. M. McGuire, D. H. McNeill, D. M. Meade, S. S. Medley, D. R. Mikkelsen, R. W. Motley, D. Mueller, Y. Murakami, J. A. Murphy, E. B. Nieschmidt, D. K. Owens, H. K. Park, A. T. Ramsey, M. H. Redi, A. L. Roquemore, P. H. Rutherford, T. Saito, N. R. Sauthoff, G. Schilling, J. Schivell, G. L. Schmidt, S. D. Scott, J. C. Sinnis, J. E. Stevens, W. Stodiek, B. C. Stratton, G. D. Tait, G. Taylor, J. R. Timberlake, H. H. Towner, M. Ulrickson, S. Von Goeler, R. M. Wieland, M. D. Williams, J. R. Wilson, K.-L. Wong, S. Yoshikawa, K. M. Young, M. C. Zarnstorf, and S. J. Zweben, in *Plasma Physics and Controlled Nuclear Fusion Research 1988*, Proceedings of the 12th International Conference, Nice (IAEA, Vienna, 1989), Vol. 1, p. 27.

²S. J. Zweben, Nucl. Fusion **29**, 825 (1989).

³R. E. Duvall, Ph.D. thesis, Princeton University, 1990.

⁴L. Chen, J. Vaclavik, and G. W. Hammett, Nucl. Fusion **28**, 389 (1988).

⁵H. E. Mynick and J. D. Strachan, Phys. Fluids **24**, 695 (1981).

⁶R. B. White and H. E. Mynick, Phys. Fluids B **1**, 980 (1989).

⁷V. Ya. Goloboroo'ko and V. A. Yavorskij, Nucl. Fusion **29**, 1025 (1989).

⁸J. D. Strachan, S. J. Zweben, C. W. Barnes, H.-S. Bosch, H. P. Furth, H. W. Hendel, D. L. Jassby, L. C. Johnson, R. W. Motley, T. Murphy, E. B. Nieschmidt, T. Saito, K. M. Young, M. G. Bell, M. Bitter, A. Cavallo, E. D. Fredrickson, K. W. Hill, H. Hsuan, D. K. Mansfield, D. R. Mikkelsen, H. K. Park, and the TFTR Group, in *Plasma Physics and Controlled Fusion Research 1988*, Nice (IAEA, Vienna, 1989), Vol. 1, p. 257.